

The Transmission Line Model for 2D Materials and van der Waals Heterostructures

Tomer Eini,¹ Anabel Atash Kahlon,¹ Matan Meshulam,^{1,2} Thomas Poirier,³
James H. Edgar,³ Seth Ariel Tongay,⁴ Yarden Mazor,¹ and Itai Epstein^{1,5,6,*}

¹*School of Electrical Engineering, Faculty of Engineering, Tel Aviv University, Tel Aviv 6997801, Israel*

²*School of Physics and Astronomy, Tel Aviv University, Tel Aviv, 6997801, Israel*

³*Tim Taylor Department of Chemical Engineering, Kansas State University, Manhattan, KS, USA*

⁴*Materials Science and Engineering, School for Engineering of Matter,*

Transport and Energy, Arizona State University, Tempe, Arizona 85287, USA

⁵*Center for Light-Matter Interaction, Tel Aviv University, Tel Aviv 6997801, Israel*

⁶*QuanTAU, Quantum Science and Technology Center, Tel Aviv University, Tel Aviv 6997801, Israel*

(Dated: July 2025)

Van der Waals heterostructures (VdWHs) composed of stacked two-dimensional (2D) materials have attracted significant attention in recent years due to their intriguing optical properties, such as strong light-matter interactions and large intrinsic anisotropy. In particular, VdWHs support a variety of polaritons hybrid quasiparticles arising from the coupling between electromagnetic waves and material excitations enabling the confinement of electromagnetic radiation to atomic scales. The ability to predict and simulate the optical response of 2D materials heterostructures is thus of high importance, being commonly performed until now via methods such as the transfer-matrix-method, or Fresnel equations. While straight forward, for complex structures these often yield long and complicated expressions, limiting intuitive and simple access to the underlying physical mechanisms that govern the optical response. In this work, we demonstrate the adaptation of the transmission line model approach for VdWHs, based on expressing the VdWH constituents by distributed electrical circuit elements described by their admittance. Since the admittance carries fundamental physical meaning of the material response to electromagnetic fields, the approach results in a one-dimensional system of propagating voltage and current waves, offering a compact and physically intuitive formulation that simplifies algebraic calculations, clarifies the conditions for existence of physical solutions, and provides valuable insight into the fundamental physical response. To demonstrate the robustness and advantages of this approach, we derive the transmission line analogs of bulk to monolayer 2D materials and show how the approach can be used to compute the reflection/transmission coefficients, polaritonic dispersion relations, and electromagnetic field distributions in a variety of 2D material VdWHs, and compare them to experimental measurements yielding very good agreement. This method provides a valuable tool for exploring and understanding the optical response of layered 2D systems.

I. INTRODUCTION

Van der Waals heterostructures (VdWHs) are structures composed of stacked layers of different two-dimensional (2D) materials, each potentially differing in thickness and composition [1, 2]. These 2D materials span a broad range of material type classification, such as semi-metallic (graphene) [3–5], dielectric (hexagonal boron nitride (hBN)) [6–8], semiconducting (transition metal dichalcogenides (TMDs)) [9–11] and more. The combination of this compositional diversity, intrinsic low dimensionality, strong quantum confinement effects, inherent anisotropy and integrability of individual 2D materials into VdWH results in unique and tunable optical response [4, 6, 12–14].

The interaction between light and 2D materials and their heterostructures has been extensively investigated, experimentally and theoretically [1, 15–20]. A central aspect of this interaction is the response of the heterostructure to impinging electromagnetic waves, resulting in

quasiparticle excitations in the material and a unique reflection/transmission response. Of particular interest in 2D materials are polaritons quasiparticles that arise from the interaction between electromagnetic fields and material excitations combining characteristics of both the photon and the material excitation [21–23], that can be studied through the analysis of electromagnetic eigenmodes in the system.

To study these type of optical and polaritonic properties of VdWHs, different methods have been applied via the analysis of Maxwells equations, such as the transfer matrix method (TMM) that relates the input and output electromagnetic fields via transmission and propagation matrices [24, 25], or the multiple reflection summation method, where the total reflection and transmission coefficients are expressed as an infinite series of round-trip contributions involving the local Fresnel coefficients at each interface [25, 26], and related techniques. While these methods are straight forward and have been commonly used in the study of light interaction with 2D material VdWHs, they often yield long and complicated analytical expressions, especially in multilayer heterostructures, which can obscure the underlying physical mechanisms of the response, giving limited intuitive insight

* itaieps@tauex.tau.ac.il

into the light-matter interaction in the heterostructure.

In this work, we propose an improved, physically informed description of the optical response of VdWHs using the framework of a transmission line model (TLM) [27–29]. In this approach, the VdWH constituents are described by distributed electrical circuit elements, characterized by their admittance. This approach is highly advantageous as the admittance carries fundamental physical meaning of the material response to electromagnetic fields. Together with the fact that it results in a one-dimensional system of propagating voltage and current waves, the TLM yields a compact and physically intuitive formulation that simplifies algebraic calculations, clarifies the conditions for existence of physical solutions, and provides valuable insight into the governing physics of the response. The TLM is a useful method due to the ability to relate between material properties and transmission line characteristics [30]. For example, [31] used the TLM to analyze the characteristics of graphene. While the TLM has been used previously in 2D material structures, the potential of this method has not been realized yet in the 2D community. To demonstrate the robustness of the TLM approach, we derive the transmission line analogs of bulk to monolayer 2D materials and their heterostructures, and compute the reflection and transmission coefficients, polaritonic dispersion relations, and electromagnetic field distributions in various VdWHs. These VdWHs include hBN-encapsulated TMD, demonstrating the effect of TMD excitons on reflection; hBN-encapsulated biased graphene, with strongly confined polaritons; and hBN encapsulated with a dielectric material, supporting hyperbolic polaritons. In addition, we show that the optical response predicted by the TLM agrees well with experimental measurements.

II. MODELING VDWHS WITH TRANSMISSION LINES

We assume a layered 2D material heterostructure constructed of uniaxial anisotropic layers (Fig. 1 (a)), such that the permittivity of the i th bulk layer is given by $\varepsilon_i = \text{diag}(\varepsilon_{i,xx}, \varepsilon_{i,xx}, \varepsilon_{i,zz})$, where $\varepsilon_{i,xx}$ and $\varepsilon_{i,zz}$ are the in-plane and out-of-plane permittivity components, respectively. Due to a symmetry in the $x-y$ plane, assuming the VdWH is infinite in that plane, we take the propagation direction to be \hat{x} and assume uniformity of the fields in the \hat{y} direction without loss of generality. A field time dependence of $e^{-i\omega t}$ is assumed as well, with a transverse dependence of e^{iqx} , where q is the x component of the wavevector (momentum), allowed due to the continuity of the transverse electric field on the boundaries between materials (see section III). The resulting fields are divided into the TM fields: $\mathbb{E} = (\hat{x}\mathbb{E}_x(z) + \hat{z}\mathbb{E}_z(z))e^{iqx}$ and $\mathbb{H} = \hat{y}\mathbb{H}_y(z)e^{iqx}$, and the TE fields: $\mathbb{H} = (\hat{x}\mathbb{H}_x(z) + \hat{z}\mathbb{H}_z(z))e^{iqx}$ and $\mathbb{E} = \hat{y}\mathbb{E}_y(z)e^{iqx}$.

Using Maxwell's equations, the above transverse electric $\mathbb{E}_T(z)$ and magnetic $\mathbb{H}_T(z)$ fields ($\mathbb{E}_x(z)$, $\mathbb{H}_y(z)$ for

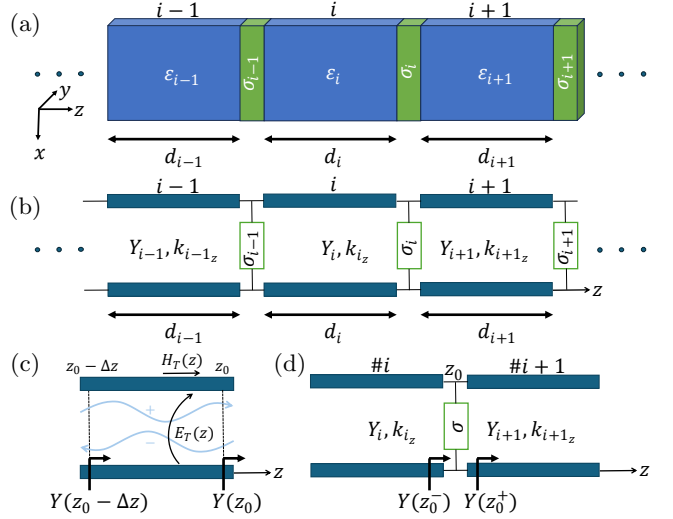


FIG. 1. Transmission line model for VdWHs. (a) A VdWH configuration constructed by layers of bulk, few-layer, or monolayer 2D materials. (b) Transmission line model of the VdWH in (a), where bulk layers are modeled as a transmission line and thin layers as a parallel admittance. (c) Transmission line model of the i th layer showing the transverse fields as analog to the voltage and current, propagating through forward and backward waves. The z dependent admittance at two different locations in the layer are marked. (d) A thin layer in the VdWH modeled as a parallel admittance between transmission lines.

TM and $\mathbb{E}_y(z)$, $-\mathbb{H}_x(z)$ for TE), satisfy the telegraph equations describing voltage $V(z)$ and current $I(z)$ in a transmission line [27–29, 32]:

$$\frac{d\mathbb{E}_T(z)}{dz} = ik_{i,z} Y_i^{-1} \mathbb{H}_T(z), \quad (1)$$

$$\frac{d\mathbb{H}_T(z)}{dz} = ik_{i,z} Y_i \mathbb{E}_T(z), \quad (2)$$

where $k_{i,z}$ is the z component of the wavevector (propagation coefficient) in the i th layer, related to the momentum by [33] $\frac{q^2}{\varepsilon_{i,zz}} + \frac{k_{i,z}^2}{\varepsilon_{i,xx}} = k_0^2$ and $q^2 + k_{i,z}^2 = \varepsilon_{i,xx} k_0^2$ for TM and TE, respectively, where k_0 is the free-space wavenumber, and Y_i is the characteristic admittance of the i th layer, equals to $\frac{\omega \varepsilon_0 \varepsilon_{i,xx}}{k_{i,z}}$ and $\frac{k_{i,z}}{\omega \mu_0}$ for TM and TE, respectively. Therefore, each bulk 2D material in the VdWH can be modeled as a transmission line (Fig 1 (b)), and the transverse electric and magnetic fields will be referred to as voltage and current in further discussions.

The transmission line supports forward (+) and backward (−) propagating waves, with a longitudinal dependence of $e^{\pm ik_{i,z} z}$, with characteristic admittance of a transmission line relating the forward or backward propagating current and voltage via

$$Y_i = \frac{\mathbb{H}_T^+(z)}{\mathbb{E}_T^+(z)} = -\frac{\mathbb{H}_T^-(z)}{\mathbb{E}_T^-(z)}. \quad (3)$$

The z dependent admittance is defined as the ratio between the current and the voltage: $Y(z) = \frac{\mathbb{H}_T(z)}{\mathbb{E}_T(z)}$. If the i th layer is half infinite for $z \rightarrow \pm\infty$, and there is no external impinging wave in the layer, then there is only a forward (or backward) propagating wave, and in this layer: $Y(z) = \pm Y_i$. The reflection coefficient at z in the i th layer is defined as:

$$r_i(z) = \frac{\mathbb{E}_T^-(z)}{\mathbb{E}_T^+(z)} = -\frac{\mathbb{H}_T^-(z)}{\mathbb{H}_T^+(z)}, \quad (4)$$

is given by:

$$r_i(z) = \frac{Y_i - Y(z)}{Y_i + Y(z)}. \quad (5)$$

The z dependent admittance at two different locations in the same i th layer is related by a tangent equation (Fig. 1 (c)). Using the z dependent admittance at the i th layer given by:

$$Y(z) = \frac{\mathbb{H}_T^+(z) + \mathbb{H}_T^-(z)}{\mathbb{E}_T^+(z) + \mathbb{E}_T^-(z)} = Y_i \frac{\mathbb{H}_T^+(z) + \mathbb{H}_T^-(z)}{\mathbb{H}_T^+(z) - \mathbb{H}_T^-(z)}, \quad (6)$$

and inserting the reflection coefficient (Eq. 4 and 5) and the z dependence of the waves into Eq. 6 at $z - \Delta z$ gives the tangent equation:

$$\begin{aligned} Y(z - \Delta z) &= Y_i \frac{\mathbb{H}_T^+(z)e^{-ik_{iz}\Delta z} + \mathbb{H}_T^-(z)e^{ik_{iz}\Delta z}}{\mathbb{H}_T^+(z)e^{-ik_{iz}\Delta z} - \mathbb{H}_T^-(z)e^{ik_{iz}\Delta z}} = \\ &= Y_i \frac{Y(z) - iY_i \tan(k_{iz}\Delta z)}{Y_i - iY(z) \tan(k_{iz}\Delta z)}. \end{aligned} \quad (7)$$

III. BOUNDARY CONDITIONS OF A THIN LAYER

Assuming a thin layer (usually a monolayer) described by its conductivity σ located at z_0 in the VdWH, and modeled as an infinitesimal layer with surface conductivity σ [34], the boundary conditions at z_0 are given by: $\mathbb{E}_T(z_0^-) = \mathbb{E}_T(z_0^+)$ and $\mathbb{H}_T(z_0^-) - \mathbb{H}_T(z_0^+) = \sigma \mathbb{E}_T(z_0)$. Note that these boundary conditions also agree with the transverse dependence introduced in section II, and in terms of admittances are given by:

$$Y(z_0^-) - Y(z_0^+) = \sigma, \quad (8)$$

the thin layer can thus be modeled as a parallel admittance between the transmission lines, as described in Fig. 1 (d).

We note that the conductivity, under the assumption of a thin layer, is related to the in-plane susceptibility of the thin layer χ_{xx} through $\sigma = -i\omega\epsilon_0\chi_{xx}d$, where $\omega = \frac{E}{\hbar}$ is the frequency and d is the thickness of the thin layer [35].

IV. REFLECTION FROM A VdWH

As an exemplary case for calculating the reflection from a VdWH using the TLM, we examine the hBN/monolayer TMD/hBN/substrate heterostructure commonly used for investigating the optical response of excitons in monolayer TMD heterostructures [36–45] (Fig. 2 (a)). Since perpendicular incidence with TM polarization was assumed, we have $k_{iz} = \sqrt{\epsilon_{i,xx}}k_0$ and $Y_i = c\epsilon_0\sqrt{\epsilon_{i,xx}}$, where c is the speed of light in vacuum. The z component of the wavevector in the hBN is denoted as k_{hBN_z} and the characteristic admittances of air, hBN and the substrate are denoted as Y_{air} , Y_{hBN} and Y_{sub} , respectively. Figure 2 (a) and (b) present the VdWH composition and TLM model, respectively. The admittance at the interface between the substrate and bottom (right) hBN layers is given by Y_{sub} , since the substrate is modeled as half infinite in the region $z > 0$. The admittance at the interface between the TMD and bottom hBN is obtained using Eq. 7

$$Y_b = Y_{hBN} \frac{Y_{sub} - iY_{hBN} \tan(k_{hBN_z}d_b)}{Y_{hBN} - iY_{sub} \tan(k_{hBN_z}d_b)}, \quad (9)$$

where d_b is the thickness of the bottom hBN. The admittance at the interface between the top (left) hBN and the TMD is given by $Y_t = Y_b + \sigma_{TMD}$, where σ_{TMD} is the conductivity of the TMD monolayer. The admittance at the interface between the air and top hBN (the entrance admittance) is given by:

$$Y_{in} = Y_{hBN} \frac{Y_t - iY_{hBN} \tan(k_{hBN_z}d_t)}{Y_{hBN} - iY_t \tan(k_{hBN_z}d_t)}, \quad (10)$$

where d_t is the thickness of the top hBN. The total reflection coefficient is therefore $r = \frac{Y_{air} - Y_{in}}{Y_{air} + Y_{in}}$.

To validate our theoretical model, we have measured the reflection coefficient from the two different VdWHs, in the first the TMD is WS_2 at $T = 4K$ above mirror gold substrate (Fig. 2 (c)) and in the second the TMD is WSe_2 at $T = 80K$ above SiO_2/Si substrate (Fig. 2 (d)). We then calculate the reflection contrast, R/R_0 , where $R = |r|^2$, $R_0 = |r_0|^2$; r and r_0 are the reflection coefficients with and without the presence of the TMD, respectively. The air above the VdWH is modeled as an additional transmission line since the top hBN has a finite thickness and the conductivity of the monolayer TMD is calculated through its in-plane susceptibility [39, 40, 46–49]:

$$\chi_{xx} = \chi_{bg} - \frac{c}{\omega_0 d_0} \frac{\gamma_r}{\omega - \omega_0 + i\frac{\gamma_{nr}}{2}}, \quad (11)$$

where χ_{bg} is the background susceptibility, ω_0 is the exciton resonance frequency, d_0 is the monolayer thickness, γ_r and γ_{nr} are the radiative and non-radiative decay rates, respectively. The susceptibility parameters are fitted to the measurements as described in [36, 37]. The contribution of the silicon in the second sample is neglected,

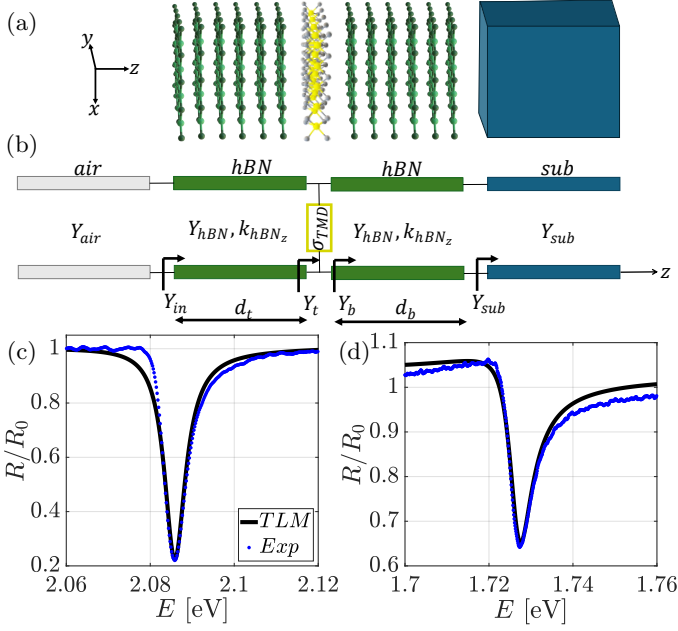


FIG. 2. Transmission line model for excitonic reflection from a WS₂ and WSe₂ VdWHs. (a) An illustration of the hBN/monolayer TMD/hBN/substrate VdWH. (b) A transmission line scheme for the configuration in (a). Measured reflection contrast (blue points) and TLM fit (black lines) for (c) the WS₂ VdWH on a gold mirror at $T = 4K$, and (d) WSe₂ VdWH on SiO₂/Si substrate at $T = 80K$.

since the parameters chosen in the experiment satisfy $|Im(k_{SiO_2})d_{SiO_2}| \gg 1$, the signal significantly decays until it reaches the SiO₂/Si interface, and therefore no significant reflection from the interface exists. Figure 2 (c) and (d) present the TLM calculated (black line) and the measured (blue points) reflection contrast for the two samples, showing good agreement.

V. TRANSVERSE RESONANCE EQUATION

The dispersion relation associated with the electromagnetic eigenmodes propagating in the VdWH, and in particular polaritons, can be found by solving the transverse resonance equation, obtained by equalizing the solutions of the z dependent admittance at a point z_0 that satisfy the boundary conditions for $z > z_0$ and $z < z_0$, when no external wave is present [28]. If the point z_0 is taken as the interface between the first and second layers in Fig. 1 (a), then the transverse resonance equation is $Y_{tot} = -Y_1$, where Y_{tot} satisfies the boundary condition for $z > z_0$. From Eq. 5 it is clear that the transverse resonance equation is equivalent for taking the total reflection coefficient to infinity $r_{tot} = \frac{Y_1 - Y_{tot}}{Y_1 + Y_{tot}} \rightarrow \infty$, as the poles of the total reflection coefficient are associated with the eigen modes of the heterostructure [50–55].

We can further simplify this formulation since polaritons are characterized by high in-plane momentum [21–

23]. This allows to approximate $q \gg \sqrt{\epsilon_{i_{zz}}}k_0$, leading to $k_{i_z} \approx iq\sqrt{\frac{\epsilon_{i_{xx}}}{\epsilon_{i_{zz}}}}$ for TM polaritons. Therefore, the characteristic admittance can be written as $Y_i = \frac{\omega\epsilon_0\epsilon_{i_{eff}}}{iq}$, where $\epsilon_{i_{eff}} = \sqrt{\epsilon_{i_{xx}}\epsilon_{i_{zz}}}$ is the effective permittivity of the i th bulk layer. A condition for the existence of polaritons in a heterostructure is that at least one of the layers has a negative real part of the permittivity (or a positive imaginary part of the conductivity) [38, 56–61].

VI. SURFACE POLARITONS IN A VdWH

As an exemplary case of obtaining a polaritonic dispersion relation, we derive the dispersion relation of graphene-exciton-polaritons (GEPs) supported by a hBN/bilayer graphene (BLG)/hBN heterostructure [58] (Fig. 3 (a)). The z dependent admittance at $z \neq 0$, where the BLG is located at $z = 0$, is given by $Y(z) = \text{sign}(z)Y_{hBN}$, since the hBN layers are half infinite for $z \rightarrow \pm\infty$. The BLG is modeled as an infinitesimal layer with conductivity σ_g , therefore $Y(0^-) - Y(0^+) = \sigma_g$, resulting in the transverse resonance equation:

$$2Y_{hBN} + \sigma_g = 0, \quad (12)$$

where $Y_{hBN} = \frac{\omega\epsilon_0\epsilon_{hBN_{eff}}}{iq}$. Assuming $\epsilon_{hBN_{eff}}$ is real and positive, which holds outside its Reststrahlen bands [62], it can be deduced that Y_{hBN} is capacitive in nature (negative imaginary admittance). Hence σ_g must be inductive (positive values of its imaginary part) in order to satisfy Eq. 12, which is enabled due to the excitonic response of the biased BLG systems [58, 63–68]. Inserting the expression of Y_{hBN} into Eq. 12 gives the known equation for a TM surface polariton in a 2D infinitesimal layer

$$q_{GEP} = \frac{2i\omega\epsilon_0\epsilon_{hBN_{eff}}}{\sigma_g}, \quad (13)$$

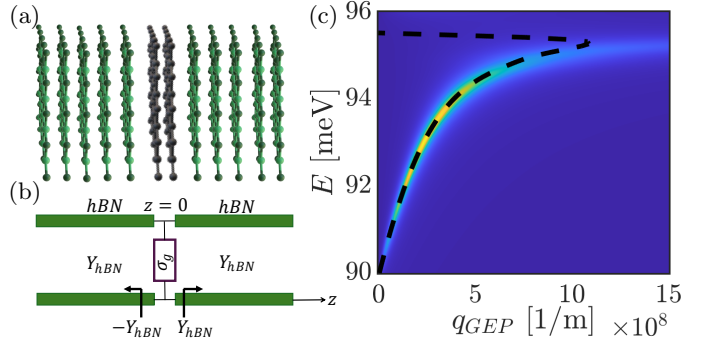


FIG. 3. Transmission line model for GEP. (a) An illustration of the hBN/BLG/hBN VdWH. (b) Transmission line schemes for the configuration. (c) Dispersion relation of GEP in the configuration, calculated from Eq. 13 (dashed black line) compared to TMM simulation (colormap).

as have been previously obtained for graphene plasmons in monolayer graphene [69] and for exciton polaritons in monolayer TMD [57, 58, 70, 71], for example, using other methods. Figure 3 (a) and (b) present the VdWH configuration and its TLM model, respectively. Figure 3 (c) compares the dispersion relation of the GEP in the VdWH calculated using Eq. 13 (dashed black line) and simulated using TMM (color map) showing excellent agreement.

VII. HYPERBOLIC POLARITONS IN A VdWH

Next we explore the response of propagating Hyperbolic-Phonon-Polaritons (HPhPs) in hBN, which have been of a large scientific interest in recent years owing to their ability to exhibit large confinement factors and low propagation losses [62, 72–74]. We derive the dispersion relation of HPhPs supported in a dielectric/hBN/dielectric heterostructure (Fig. 4 (a)) using the equivalent TLM presented in Fig. 4 (b), while previous approaches have used Fresnel equations and ray-based methods [62, 74], for example. The z dependent admittance at $|z| > \frac{d_{hBN}}{2}$, where the hBN is located at $|z| < \frac{d_{hBN}}{2}$, is given by $Y(z) = \text{sign}(z)Y_d$, where Y_d is the characteristic admittance of the dielectric, since the dielectric layers are half infinite for $z \rightarrow \pm\infty$. Using Eq. 7 to relate between $Y(\frac{d_{hBN}}{2})$ and $Y(-\frac{d_{hBN}}{2})$ we get:

$$-Y_d = Y_{hBN} \frac{Y_d - iY_{hBN} \tan(k_{hBNz} d_{hBN})}{Y_{hBN} - iY_d \tan(k_{hBNz} d_{hBN})}. \quad (14)$$

By setting $Y_{hBN} = \frac{\omega \varepsilon_0 \varepsilon_{hBN_{eff}}}{iq}$, $Y_d = \frac{\omega \varepsilon_0 \varepsilon_{d_{eff}}}{iq}$ and $k_{hBNz} \approx iq \sqrt{\frac{\varepsilon_{hBN_{xx}}}{\varepsilon_{hBN_{zz}}}}$, after some algebra we obtain the known dispersion relation of hyperbolic polaritons, as previously obtained for HPhPs and Hyperbolic-Exciton-polaritons using other methods [57, 62]:

$$q_{HPhP} = \frac{i}{d_{hBN}} \sqrt{\frac{\varepsilon_{hBN_{zz}}}{\varepsilon_{hBN_{xx}}}} \left[2 \arctan \left(i \frac{\varepsilon_{d_{eff}}}{\varepsilon_{hBN_{eff}}} \right) + \pi L \right], \quad (15)$$

where L is the modal order.

Due to the symmetry of the VdWH around the z axis, it supports even modes (even voltage around the z axis) and odd modes (odd voltage around the z axis). We note that the parity of the current is opposite to the parity of the voltage in TM polarization. We can use this symmetry to obtain more easily the dispersion relation in Eq. 15.

Since the transverse fields are continuous at $z = 0$, the even modes satisfy a nullification of the current at $z = 0$ and $Y(z = 0) = 0$ and the odd modes satisfy a nullification of the voltage at $z = 0$ and $Y^{-1}(z = 0) = 0$. Applying these conditions to Eq. 14, we obtain for the even modes $Y_{air} - iY_{hBN} \tan(k_{even, hBNz} \frac{d_{hBN}}{2}) = 0$ and for the odd modes

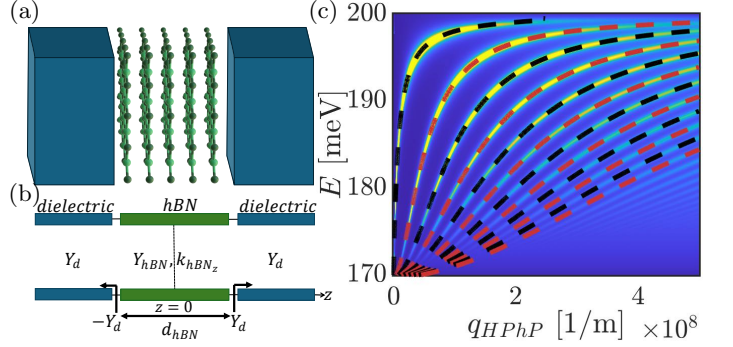


FIG. 4. Transmission line model for HPhP. (a) An illustration of the dielectric/hBN/dielectric VdWH. (b) Transmission line schemes for the configuration in (a). (c) Dispersion relation of HPhP in the configuration, calculated from Eq. 15 (dashed black line for even modes and dashed red line for odd modes) compared to TMM simulation (colormap).

is given by $Y_{hBN} - iY_{air} \tan(k_{odd, hBNz} \frac{d_{hBN}}{2}) = 0$. From these equations, the dispersion relation in Eq. 15 can be obtained, with even modal orders for the even modes and odd modal orders for the odd modes.

Figure 4 (c) compares the dispersion relation of the HPhP in the VdWH calculated using Eq. 15 (dashed black line for even modes and dashed red line for odd modes) and simulated using the TMM (colormap), showing very well agreement.

As another robust example of using the TLM to analyze the hyperbolic response of a VdWH, we note that Kats et. al. [71] have recently shown that an alternating TMD monolayers and hBN layered VdWH exhibits a hyperbolic response, by analyzing the reflection and polaritonic properties of the structure as obtained from TLM approach.

VIII. POLARITONS HYBRIDIZATION IN A VdWH

To demonstrate the advantage of the TLM in the study of polaritons in VdWHs, we show the TLM analysis of a dielectric/hBN/BLG/hBN/dielectric VdWH, which supports both HPhPs and graphene excitons [59] (Fig. 5 (a)), and where the physical meaning of the admittances plays an important role. The equivalent TLM of the VdWH is presented in Fig. 5 (b). The numerical simulation of the TMM (colormap in Fig. 5 (c) and (d)) shows multiple modes, branches and anti-crossings. The derivation of an analytical expression of the dispersion relation and field distributions for such a complicated modal picture is very challenging via the TMM, or similar approaches, hindering the underlying physics of the system. Nevertheless, the TLM approach offers much simpler derivations that allow to understand the physical properties of the system. We start with the analysis of a symmetric structure with both hBN layers having a

thickness of $d_t = d_b$. Due to the symmetry of the VdWH, it supports even and odd modes. Since the odd modes satisfy a nullification of the voltage at $z = 0$, yielding no surface current on the bilayer graphene, the magnetic field is continuous and the odd modes are not affected by the presence of the BLG (dashed red line in Fig. 5 (c)). The even modes (dashed purple line) present an anti-crossing between the even modes of HPhPs (black line) and the exciton energies of the BLG (dashed white

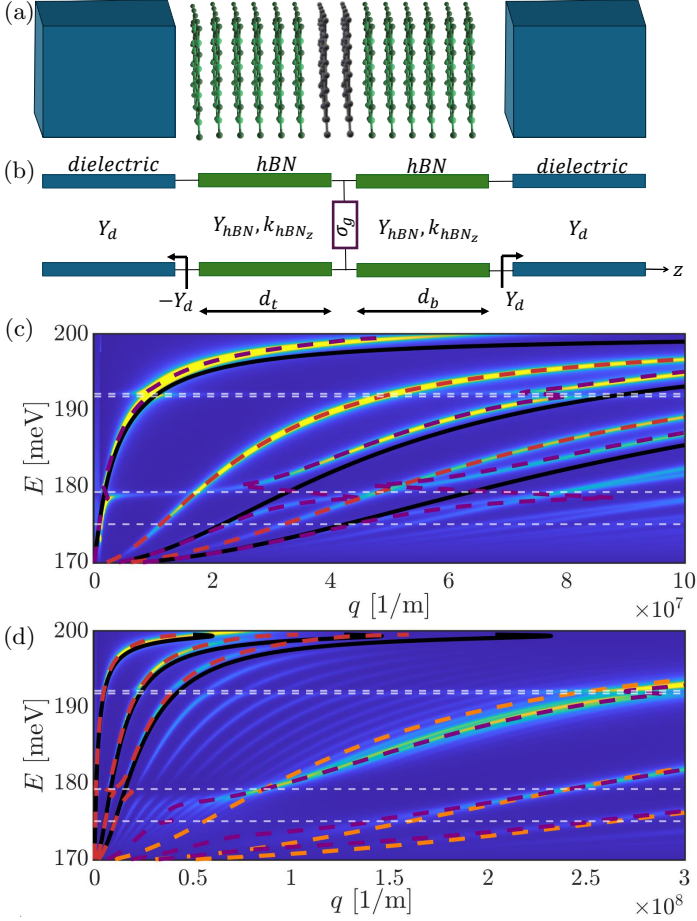


FIG. 5. Transmission line model for hybridized polaritons. (a) An illustration of the dielectric/hBN/BLG/hBN/dielectric VdWH. (b) Transmission line schemes for the configuration in (a). (c) Dispersion relation of the hybridized polaritons in the configuration in the symmetric structure, (dashed purple line for even modes and dashed red line for odd modes) compared to TMM simulation (colormap). Even modes of HPhP for hBN with thickness of $d_b + d_t$ (black lines) and exciton energies of BLG (dashed white lines) are also plotted. (d) Dispersion relation of the hybridized polaritons in the configuration in the asymmetric structure, (dashed red line for the low momentum modes and dashed purple line for the high momentum modes) compared to TMM simulation (colormap). Modes of HPhP for hBN with thickness of $d_b + d_t$ (black lines), odd modes of HPhP for hBN with thickness of $2d_t$ (dashed orange lines), and exciton energies of BLG (dashed white lines) are also plotted.

line), forming hybridized polaritons. The dispersion relation can be found using the TLM with the assumption that the conductivity of the BLG is much smaller than the characteristic admittance of the hBN, $|\sigma| \ll |Y_{hBN}|$ [59] (Fig. 5 (c)).

Next, we analyze an asymmetric structure with $d_t \ll d_b$, which supports two sets of modes with either low momentum and high momentum (Fig. (d)). The low momentum modes (dashed red line) present an anti-crossing between modes of HPhP (black line) and the exciton energies (dashed white line), since they satisfy $|\sigma| \ll |Y_{hBN}|$, and can be found using the TLM, similarly to the symmetric case. The high momentum modes, however, satisfy $|\sigma| \gg |Y_{hBN}|$, meaning that the graphene serves almost as a short circuit and therefore can be approximately described as a PEC, separating between the top and bottom hBN layers. Since d_b is larger than all quantities with length dimensions, the bottom layer can be approximated as half infinite. We hence approximately receive odd modes of HPhPs with of thickness $2d_t$ (dashed orange line), where the more accurate dispersion relation can be derived using the TLM by keeping another order of $|\frac{Y_{hBN}}{\sigma}|$ [59] (dashed purple line). Thus, the TLM approach enables to obtain analytical expressions of the hybridized polaritons in the VdWH, using the physical properties of the admittances in the system and the basic physical principle of symmetry.

IX. FIELD DISTRIBUTION

Next we show how the field distributions in the VdWHs can be easily obtained using the TLM method. The voltage in the i th layer is given by:

$$\mathbb{E}_T(z) = \mathbb{E}_T^+(z_i)e^{ik_{iz}(z-z_i)}[1 + r(z_{i+1})e^{-ik_{iz}(z-z_{i+1})}], \quad (16)$$

where z_i and z_{i+1} are arbitrary locations in the i th layer, could be chosen as the interfaces between the $i \mp 1$ th and i th layers for convenience, and $\mathbb{E}_T^+(z_i)$ is an amplitude defined as the forward propagating voltage at z_i . The reflection coefficients can be calculated using Eq. 5, where the characteristic and the z dependent admittances are usually already calculated previously in order to find the total reflection coefficient or the dispersion relation of the polaritons in the VdWH. If there is an external impinging wave then it determines the amplitude in the first layer, while the amplitudes in the other layers can be found using the continuity of the voltage. If one is interested in finding the field distribution of the polaritons, then there is no impinging wave, and the field can be found up to an arbitrary constant. The current can be found directly from the voltage by multiplying it by $Y(z)$, or by multiplying each propagating wave in each layer separately by $\pm Y_i$ and the longitudinal field can be derived from the transverse field using Maxwell's equations.

CONCLUSIONS

In conclusion, we have shown that the interaction of VdWHs with light can be appropriately modeled using an equivalent TLM. We derived the TLM for bulk to monolayer 2D materials, composing VdWHs, obtaining reflection coefficients agreeing well with experimental results, and polariton dispersion relations with excellent agreement compared to numerical simulations. We used the TLM to gain physical insight on the optical and polaritonic response of VdWHs. This method can be used in future theoretical studies of interaction between light and VdWHs, enabling exploring and understanding physical phenomena of the interaction.

METHODS

The VdWHs investigated in this study were assembled via a dry transfer process, as detailed in Ref. [75]. Reflection measurements were performed by focusing a broadband light source onto the VdWHs through an ob-

jective lens. The reflected signal was collected by the same objective and then routed into a spectrometer for spectral analysis. The reflection signal R was acquired from a region containing the complete hBN/TMD/hBN structure, whereas the reference signal R_0 was measured from an adjacent area in which the TMD layer was absent.

ACKNOWLEDGMENTS

I.E. acknowledges the Israeli Science Foundation personal grant number 865/24, the Ministry of Science and Technology grant number 0005757, and the support of the European Union (ERC, TOP-BLG, Project No. 101078192). Y. M. acknowledges the support of ISF Grant No. 1089/22. J.H.E. acknowledge support from the Office of Naval Research under award no. N00014-20-1-2474 for hBN crystal growth. S.T acknowledges primary support from DOE-SC0020653 (excitonic testing) and NSF CBET 2330110 (environmental stabilization), and support from Applied Materials Inc., and Lawrence Semiconductor Labs for material development / initial characterization.

-
- [1] A. K. Geim and I. V. Grigorieva, Van der Waals heterostructures, *Nature* **499**, 419 (2013).
 - [2] A. Castellanos-Gomez, X. Duan, Z. Fei, H. R. Gutierrez, Y. Huang, X. Huang, J. Qereda, Q. Qian, E. Sutter, and P. Sutter, Van der Waals heterostructures, *Nature Reviews Methods Primers* 2022 2:1 **2**, 1 (2022).
 - [3] A. K. Geim and K. S. Novoselov, The rise of graphene, *Nature Materials* **6**, 183 (2007).
 - [4] A. N. Grigorenko, M. Polini, and K. S. Novoselov, Graphene plasmonics, *Nature Photonics* 2012 6:11 **6**, 749 (2012).
 - [5] A. K. Geim, Graphene: Status and Prospects, *Science* **324**, 1530 (2009).
 - [6] J. D. Caldwell, I. Aharonovich, G. Cassaboiss, J. H. Edgar, B. Gil, and D. N. Basov, Photonics with hexagonal boron nitride, *Nature Reviews Materials* 2019 4:8 **4**, 552 (2019).
 - [7] K. Zhang, Y. Feng, F. Wang, Z. Yang, and J. Wang, Two dimensional hexagonal boron nitride (2D-hBN): synthesis, properties and applications, *Journal of Materials Chemistry C* **5**, 11992 (2017).
 - [8] A. Zunger, A. Katzir, and A. Halperin, Optical properties of hexagonal boron nitride, *Physical Review B* **13**, 5560 (1976).
 - [9] S. Manzeli, D. Ovchinnikov, D. Pasquier, O. V. Yazyev, and A. Kis, 2D transition metal dichalcogenides, *Nature Reviews Materials* 2017 2:8 **2**, 1 (2017).
 - [10] Q. H. Wang, K. Kalantar-Zadeh, A. Kis, J. N. Coleman, and M. S. Strano, Electronics and optoelectronics of two-dimensional transition metal dichalcogenides, *Nature Nanotechnology* **7**, 699 (2012).
 - [11] W. Choi, N. Choudhary, G. H. Han, J. Park, D. Akinwande, and Y. H. Lee, Recent development of two-dimensional transition metal dichalcogenides and their applications, *Materials Today* **20**, 116 (2017).
 - [12] F. Xia, H. Wang, D. Xiao, M. Dubey, and A. Ramasubramaniam, Two-dimensional material nanophotonics, *Nature Photonics* **8**, 899 (2014).
 - [13] G. Wang, A. Chernikov, M. M. Glazov, T. F. Heinz, X. Marie, T. Amand, and B. Urbaszek, Colloquium: Excitons in atomically thin transition metal dichalcogenides, *Reviews of Modern Physics* **90**, 021001 (2018).
 - [14] J. D. Caldwell, L. Lindsay, V. Giannini, I. Vurgaftman, T. L. Reinecke, S. A. Maier, and O. J. Glembocki, Low-loss, infrared and terahertz nanophotonics using surface phonon polaritons, *Nanophotonics* **4**, 44 (2015).
 - [15] T. Deilmann, M. Rohlfing, and U. Wurstbauer, Light-matter interaction in van der Waals hetero-structures, *Journal of Physics: Condensed Matter* **32**, 333002 (2020).
 - [16] C. Schneider, M. M. Glazov, T. Korn, S. Höfling, and B. Urbaszek, Two-dimensional semiconductors in the regime of strong light-matter coupling, *Nature Communications* 2018 9:1 **9**, 1 (2018).
 - [17] F. H. Koppens, T. Mueller, P. Avouris, A. C. Ferrari, M. S. Vitiello, and M. Polini, Photodetectors based on graphene, other two-dimensional materials and hybrid systems, *Nature Nanotechnology* 2014 9:10 **9**, 780 (2014).
 - [18] D. Akinwande, C. Huyghebaert, C. H. Wang, M. I. Serna, S. Goossens, L. J. Li, H. S. Wong, and F. H. Koppens, Graphene and two-dimensional materials for silicon technology, *Nature* 2019 573:7775 **573**, 507 (2019).
 - [19] A. C. Ferrari, F. Bonaccorso, V. Fal'ko, K. S. Novoselov, S. Roche, P. Bøggild, S. Borini, F. H. Koppens, V. Palermo, N. Pugno, and et al., Science and technology roadmap for graphene, related two-dimensional crystals, and hybrid systems, *Nanoscale* **7**, 4598 (2015).

- [20] F. J. G. de Abajo, D. N. Basov, F. H. L. Koppens, L. Orsini, M. Ceccanti, S. Castilla, L. Cavicchi, M. Polini, P. A. D. Gonçalves, A. T. Costa, and et al., Roadmap for Photonics with 2D Materials, arXiv:2504.04558 10.1021/acsphotonics.5c00353 (2025).
- [21] D. N. Basov, M. M. Fogler, and F. J. García De Abajo, Polaritons in van der Waals materials, *Science* **354**, 10.1126/SCIENCE.AAG1992 (2016).
- [22] T. Low, A. Chaves, J. D. Caldwell, A. Kumar, N. X. Fang, P. Avouris, T. F. Heinz, F. Guinea, L. Martin-Moreno, and F. Koppens, Polaritons in layered two-dimensional materials, *Nature Materials* 2016 16:2 **16**, 182 (2016).
- [23] D. N. Basov, A. Asenjo-Garcia, P. J. Schuck, X. Zhu, and A. Rubio, Polariton panorama, *Nanophotonics* **10**, 549 (2021).
- [24] T. Zhan, X. Shi, Y. Dai, X. Liu, and J. Zi, Transfer matrix method for optics in graphene layers, *Journal of Physics: Condensed Matter* **25**, 215301 (2013).
- [25] M. Born and E. Wolf, Principles of Optics: Electromagnetic Theory of Propagation, Interference and Diffraction of Light.
- [26] W. Cho Chew, *Waves and Fields in Inhomogenous Media* (IEEE Xplore, 1995).
- [27] David k Cheng, field-and-wave-electromagnetics.
- [28] Pozar D.M., *Microwave Engineering* (2011).
- [29] S. A. Schelkunoff, Transmission theory of plane electromagnetic waves, *IEEE Xplore* **25**, 1457 (1937).
- [30] N. Marcuvitz, *Waveguide Handbook* (let, 1951).
- [31] H. J. Lee, E. Kim, J. G. Yook, and J. Jung, Intrinsic characteristics of transmission line of graphenes at microwave frequencies, *Applied Physics Letters* **100**, 223102 (2012).
- [32] L. B. Felsen and N. Marcuvitz, *Radiation and Scattering of Waves* (John Wiley & Sons, 1994).
- [33] L. Ferrari, C. Wu, D. Lepage, X. Zhang, and Z. Liu, Hyperbolic metamaterials and their applications, *Progress in Quantum Electronics* **40**, 1 (2015).
- [34] G. W. Hanson, Dyadic Green's functions and guided surface waves for a surface conductivity model of graphene, *Journal of Applied Physics* **103**, 64302 (2008).
- [35] T. B. A. Senior and J. L. Volakis, *Approximate Boundary Conditions in Electromagnetics* (1995).
- [36] A. A. Kahlon, M. Meshulam, T. Eini, T. Poirier, J. H. Edgar, S. A. Tongay, and I. Epstein, Importance of pure dephasing in the optical response of excitons in high-quality van der Waals heterostructures, *Physical Review B* **112**, L041402 (2025).
- [37] I. Epstein, . Bernat, T. Terres, . Andrej, A. Chaves, V.-V. Pusapati, D. A. Rhodes, B. Frank, V. Zimmermann, Y. Qin, K. Watanabe, T. Taniguchi, H. Giessen, S. Tongay, J. C. Hone, N. M. R. Peres, and F. H. L. Koppens, Near-Unity Light Absorption in a Monolayer WS₂ Van der Waals Heterostructure Cavity, *Nano Letters* 10.1021/acs.nanolett.0c00492 (2020).
- [38] I. Epstein, A. J. Chaves, D. A. Rhodes, B. Frank, K. Watanabe, T. Taniguchi, H. Giessen, J. C. Hone, N. M. Peres, and F. H. Koppens, Highly confined in-plane propagating exciton-polaritons on monolayer semiconductors, *2D Materials* **7**, 035031 (2020).
- [39] J. Horng, E. W. Martin, Y. H. Chou, E. Courtade, T. C. Chang, C. Y. Hsu, M. H. Wentzel, H. G. Ruth, T. C. Lu, S. T. Cundiff, F. Wang, and H. Deng, Perfect absorption by an atomically thin crystal, *Physical Review Applied* **14**, 024009 (2020).
- [40] C. Robert, M. A. Semina, F. Cadiz, M. Manca, E. Courtade, T. Taniguchi, K. Watanabe, H. Cai, S. Tongay, B. Lassagne, P. Renucci, T. Amand, X. Marie, M. M. Glazov, and B. Urbaszek, Optical spectroscopy of excited exciton states in MoS₂ monolayers in van der Waals heterostructures, *Physical Review Materials* **2**, 011001 (2018).
- [41] C. Rogers, D. Gray, N. Bogdanowicz, T. Taniguchi, K. Watanabe, and H. Mabuchi, Coherent feedback control of two-dimensional excitons, *Physical Review Research* **2**, 012029 (2020).
- [42] M. Li, S. Biswas, C. U. Hail, and H. A. Atwater, Refractive Index Modulation in Monolayer Molybdenum Diselenide, *Nano Letters* **21**, 7602 (2021).
- [43] P. A. Gonçalves, L. P. Bertelsen, S. Xiao, and N. A. Mortensen, Plasmon-exciton polaritons in two-dimensional semiconductor/metal interfaces, *Physical Review B* **97**, 041402 (2018).
- [44] O. A. Ajayi, J. V. Ardelean, G. D. Shepard, J. Wang, A. Antony, T. Taniguchi, K. Watanabe, T. F. Heinz, S. Strauf, X.-Y. Zhu, and J. C. Hone, Approaching the intrinsic photoluminescence linewidth in transition metal dichalcogenide monolayers, *2D Materials* **4**, 031011 (2017).
- [45] F. Cadiz, E. Courtade, C. Robert, G. Wang, Y. Shen, H. Cai, T. Taniguchi, K. Watanabe, H. Carrere, D. Lagarde, M. Manca, T. Amand, P. Renucci, S. Tongay, X. Marie, and B. Urbaszek, Excitonic Linewidth Approaching the Homogeneous Limit in MoS₂-Based van der Waals Heterostructures, *Physical Review X* **7**, 021026 (2017).
- [46] Y. Li, A. Chernikov, X. Zhang, A. Rigosi, H. M. Hill, A. M. van der Zande, D. A. Chenet, E.-M. Shih, J. Hone, and T. F. Heinz, Measurement of the optical dielectric function of monolayer transition-metal dichalcogenides, *PHYSICAL REVIEW B* **90**, 205422 (2014).
- [47] G. Scuri, Y. Zhou, A. A. High, D. S. Wild, C. Shu, K. D. Greve, L. A. Jauregui, T. Taniguchi, K. Watanabe, P. Kim, M. D. Lukin, and H. Park, Large Excitonic Reflectivity of Monolayer MoSe₂ Encapsulated in Hexagonal Boron Nitride, *Physical Review Letters* **120**, 037402 (2018).
- [48] P. Back, S. Zeytinoglu, A. Ijaz, M. Kroner, and A. Imamolu, Realization of an Electrically Tunable Narrow-Bandwidth Atomically Thin Mirror Using Monolayer MoSe₂, *Physical Review Letters* **120**, 037401 (2018).
- [49] E. Shahmoon, D. S. Wild, M. D. Lukin, and S. F. Yelin, Cooperative Resonances in Light Scattering from Two-Dimensional Atomic Arrays, *Physical Review Letters* **118**, 113601 (2017).
- [50] F. Alpeggiani, N. Parappurath, E. Verhagen, and L. Kuipers, Quasinormal-mode expansion of the scattering matrix, *Physical Review X* **7**, 021035 (2017).
- [51] P. T. Leung, S. Y. Liu, and K. Young, Completeness and orthogonality of quasinormal modes in leaky optical cavities, *Physical Review A* **49**, 3057 (1994).
- [52] E. A. Muljarov, W. Langbein, and R. Zimmermann, Brillouin-Wigner perturbation theory in open electromagnetic systems, *Europhysics Letters* **92**, 50010 (2011).
- [53] P. T. Kristensen, C. V. Vlack, and S. Hughes, Generalized effective mode volume for leaky optical cavities, *Optics Letters*, Vol. 37, Issue 10, pp. 1649-1651 **37**, 1649 (2012).

- [54] C. Sauvan, J. P. Hugonin, I. S. Maksymov, and P. Lalanne, Theory of the spontaneous optical emission of nanosize photonic and plasmon resonators, *Physical Review Letters* **110**, 237401 (2013).
- [55] E. A. Muljarov and W. Langbein, Resonant-state expansion of dispersive open optical systems: Creating gold from sand, *Physical Review B* **93**, 075417 (2016).
- [56] S. A. Maier, *PLASMONICS: FUNDAMENTALS AND APPLICATIONS*.
- [57] T. Eini, T. Asherov, Y. Mazor, and I. Epstein, Valley-polarized hyperbolic exciton polaritons in few-layer two-dimensional semiconductors at visible frequencies, *Physical Review B* **106**, L201405 (2022).
- [58] T. Eini, M. M. Quintela, J. Henriques, R. Ribeiro, Y. Mazor, N. Peres, and I. Epstein, Electrically Tunable Interband Collective Excitations in Biased Bilayer and Trilayer Graphene, *Physical Review Letters* **134**, 196903 (2025).
- [59] T. Eini, N. M. R. Peres, Y. Mazor, and I. Epstein, Exciton-hyperbolic-phonon-polariton Hybridization in Biased Bilayer Graphene, arXiv:2506.04796 (2025).
- [60] A. J. Sternbach, S. H. Chae, S. Latini, A. A. Rikhter, Y. Shao, B. Li, D. Rhodes, B. Kim, P. J. Schuck, X. Xu, X.-Y. Zhu, R. D. Averitt, J. Hone, M. M. Fogler, A. Rubio, and D. N. Basov, Programmable hyperbolic polaritons in van der Waals semiconductors, *Science* **371**, 617 (2021).
- [61] Y. Li, A. Chernikov, X. Zhang, A. Rigosi, H. M. Hill, A. M. Van Der Zande, D. A. Chenet, E. M. Shih, J. Hone, and T. F. Heinz, Measurement of the optical dielectric function of monolayer transition-metal dichalcogenides: MoS₂, Mo S e₂, WS₂, and WS e₂, *Physical Review B - Condensed Matter and Materials Physics* **90**, 205422 (2014).
- [62] S. Dai, Z. Fei, Q. Ma, A. S. Rodin, M. Wagner, A. S. McLeod, M. K. Liu, W. Gannett, W. Regan, K. Watanabe, T. Taniguchi, M. Thiemens, G. Dominguez, A. H. Castro Neto, A. Zettl, F. Keilmann, P. Jarillo-Herrero, M. M. Fogler, and D. N. Basov, Tunable phonon polaritons in atomically thin van der Waals crystals of boron nitride, *Science* **343**, 1125 (2014).
- [63] C. H. Park and S. G. Louie, Tunable excitons in biased bilayer graphene, *Nano Letters* **10**, 426 (2010).
- [64] T. Cao, M. Wu, and S. G. Louie, Unifying Optical Selection Rules for Excitons in Two Dimensions: Band Topology and Winding Numbers, *Physical Review Letters* **120**, 087402 (2018).
- [65] L. Ju, L. Wang, T. Cao, T. Taniguchi, K. Watanabe, S. G. Louie, F. Rana, J. Park, J. Hone, F. Wang, and P. L. McEuen, Tunable excitons in bilayer graphene, *Science* **358**, 907 (2017).
- [66] L. Ju, L. Wang, X. Li, S. Moon, M. Ozerov, Z. Lu, T. Taniguchi, K. Watanabe, E. Mueller, F. Zhang, D. Smirnov, F. Rana, and P. L. McEuen, Unconventional valley-dependent optical selection rules and Landau level mixing in bilayer graphene, *Nature Communications* 2020 11:1 **11**, 1 (2020).
- [67] J. C. Henriques, I. Epstein, and N. M. Peres, Absorption and optical selection rules of tunable excitons in biased bilayer graphene, *Physical Review B* **105**, 045411 (2022).
- [68] M. F. Quintela and N. M. Peres, Tunable excitons in rhombohedral trilayer graphene, *Physical Review B* **105**, 205417 (2022).
- [69] P. A. D. Gonçalves and N. M. R. Peres, An Introduction to Graphene Plasmonics, *An Introduction to Graphene Plasmonics*, 1 (2016).
- [70] I. Epstein, A. J. Chaves, D. A. Rhodes, B. Frank, K. Watanabe, T. Taniguchi, H. Giessen, J. C. Hone, N. M. R. Peres, and F. H. L. Koppens, Highly confined in-plane propagating exciton-polaritons on monolayer semiconductors, *2D Materials* **7**, 035031 (2020).
- [71] I. Kats, T. Eini, and I. Epstein, Monolayer semiconductor superlattices as hyperbolic materials at visible to near-infrared frequencies, *Physical Review B* **111**, L041302 (2025).
- [72] J. D. Caldwell, A. V. Kretinin, Y. Chen, V. Giannini, M. M. Fogler, Y. Francescato, C. T. Ellis, J. G. Tischler, C. R. Woods, A. J. Giles, M. Hong, K. Watanabe, T. Taniguchi, S. A. Maier, and K. S. Novoselov, Sub-diffractive volume-confined polaritons in the natural hyperbolic material hexagonal boron nitride, *Nature Communications* 2014 5:1 **5**, 1 (2014).
- [73] P. Li, M. Lewin, A. V. Kretinin, J. D. Caldwell, K. S. Novoselov, T. Taniguchi, K. Watanabe, F. Gaussmann, and T. Taubner, Hyperbolic phonon-polaritons in boron nitride for near-field optical imaging and focusing, *Nature Communications* 2015 6:1 **6**, 1 (2015).
- [74] Z. Zheng, J. Chen, Y. Wang, X. Wang, X. Chen, P. Liu, J. Xu, W. Xie, H. Chen, S. Deng, and N. Xu, Highly Confined and Tunable Hyperbolic Phonon Polaritons in Van Der Waals Semiconducting Transition Metal Oxides, *Advanced Materials* **30**, 1705318 (2018).
- [75] A. Castellanos-Gomez, M. Buscema, R. Molenaar, V. Singh, L. Janssen, H. S. Van Der Zant, and G. A. Steele, Deterministic transfer of two-dimensional materials by all-dry viscoelastic stamping, *2D Materials* **1**, 011002 (2014).